# SPATIAL SIGMA-DELTA MODULATION FOR THE MASSIVE MIMO DOWNLINK

Mingjie Shao<sup>†</sup>, Wing-Kin Ma<sup>†</sup>, Qiang Li<sup>‡</sup> and Lee Swindlehurst\*

<sup>†</sup> Department of Electronic Engineering, The Chinese University of Hong Kong, Hong Kong SAR, China <sup>‡</sup> School of Information and Communication Engineering, University of Electronic Science and Technology of China <sup>\*</sup> Center for Pervasive Communications and Computing, University of California Irvine, Irvine, CA 92697, USA

#### ABSTRACT

In massive MIMO, replacing high-resolution ADCs/DACs with low-resolution ones has been deemed as a potential way to significantly reduce the power consumption and hardware costs of massive MIMO implementations. In this context, the challenge lies in how the quantization error effect can be suppressed under low-resolution ADCs/DACs. In this paper we study a spatial sigma-delta ( $\Sigma\Delta$ ) modulation approach for massive MIMO downlink precoding under one-bit DACs.  $\Sigma\Delta$  modulation is a classical signal processing concept for coarse analog-to-digital/digital-to-analog conversion of temporal signals. Fundamentally its idea is to shape the quantization error as high-frequency noise and to avoid using the high-frequency region by oversampling. Assuming a uniform linear array at the base station (BS), we show how  $\Sigma\Delta$  modulation can be adapted to the space, or MIMO, case. Essentially, by relating frequency in the temporal case and angle in the spatial case, we develop a spatial  $\Sigma\Delta$  modulation solution. By considering sectored array operations we study how the quantization error effect can be reduced, and the effective SNR improved, for zero-forcing (ZF) precoding. Our simulation results show that ZF precoding under spatial  $\Sigma\Delta$  modulation performs much better than ZF precoding under direct quantization.

*Index Terms*— massive MIMO, spatial sigma-delta modulation, one-bit precoding

### 1. INTRODUCTION

Recently, coarsely quantized signal processing techniques are flourishing in studies of massive multi-input multi-output (MIMO) transceiver implementations. These studies are strongly motivated by the need to reduce the hardware cost and power consumption of radio-frequency (RF) front-ends—which grow rapidly under massive MIMO—and the idea is to use low-resolution analog-to-digital converters (ADCs)/digital-to-analog converters (DACs) and energy-efficient low-dynamic-range power amplifiers. A number of researchers have investigated MIMO channel estimation and MIMO detection using one-bit or low-resolution ADCs [2–8], and it has been found that the very large number of antennas in massive MIMO indeed helps recover information lost due to the coarsely quantized signals.

MIMO precoding using one-bit DACs is another emerging topic in this area. A natural direction is to simply quantize the output of a conventional linear precoder, such as that of the zero forcing (ZF) precoder, and the question is how the coarse quantization effects impact system performance [9–11] using, for example, the Bussgang decomposition as an analysis tool. More recently, there has been emphasis on directly designing a one-bit precoder, rather than follow-

This paper is an abridged version of [1].

ing the aforementioned precode-then-quantize approach. The direct one-bit precoding designs use criteria such as minimum mean-square error and minimum symbol error probability [12–19], and numerically these designs were found to yield significantly improved performance. The challenge with the direct one-bit precoding designs is mainly with the complicated large-scale integer optimization problem.

More recently, the idea of spatial  $\Sigma\Delta$  modulation has been exploited in massive MIMO transceiver designs. Temporal  $\Sigma\Delta$  modulation is a classic quantization technique for oversampled signals. The  $\Sigma\Delta$  principle is to employ a feedback loop to quantize the accumulated error between the input and the one-bit quantized output. The net effect is to shape the quantization noise to the high end of the frequency spectrum, where it can be separated from the signal of interest using a simple low-pass filter and decimator; see [20] for details. Alternatively, one can employ the  $\Sigma\Delta$  effect using signals oversampled in space using an array of antennas. In such spatial  $\Sigma\Delta$  architectures, the feedback signal is derived from the delayed and quantized outputs of adjacent antennas. Oversampling in this context means that the elements of a uniform linear array would be spaced closer than one-half wavelength apart. As a result, the quantization error can be pushed to higher spatial frequencies, mitigating the distortion for signals of interest that might arrive from lower spatial frequencies, i.e., those near the broadside of the array. This idea has been exploited recently by a number of researchers for signal detection [21–24], channel estimation [25] and spectral efficiency [26] in the uplink. However, the use of spatial  $\Sigma\Delta$  modulation for the downlink has received much less attention [27, 28].

This paper explores what opportunities spatial  $\Sigma\Delta$  modulation can bring in the context of one-bit massive MIMO precoding. Our study reveals that one-bit massive MIMO precoding using spatial  $\Sigma\Delta$  modulation, or simply  $\Sigma\Delta$  precoding for short, allows us to effectively mitigate the quantization noise effects. More precisely, we consider uniform linear arrays with user angles lying within a sector near broadside, where the quantization noise can be substantially suppressed when the number of antennas is large. Moreover, we propose a ZF precoder under  $\Sigma\Delta$  modulation. The effective SNR analysis suggests that  $\Sigma\Delta$  ZF is quite suitable for massive MIMO systems. Simulation results demonstrate that the performance of  $\Sigma\Delta$  ZF is much better than that of the directly quantized ZF. Also,  $\Sigma\Delta$  ZF shows competitive performance compared to existing direct one-bit designs that require complicated optimization.

### 2. PROBLEM SETTINGS

We consider the multiuser MISO downlink over a quasi-static frequency-flat channel and under one-bit transmitted signal con-

straints. The model is given by

$$y_{i,t} = \sqrt{\frac{P}{2N}} \boldsymbol{h}_i^T \boldsymbol{x}_t + v_{i,t}, \quad t = 1, \dots, T,$$
 (1)

for  $i=1,\ldots,K$ , where  $y_{i,t}\in\mathbb{C}$  represents the complex baseband received signal of the ith user at symbol time t; K denotes the number of users; T is the transmission block length; P is the total transmission power; N is the number of antennas of the base station (BS);  $h_i\in\mathbb{C}^N$  is the channel from the BS to the ith user;  $\sqrt{P/(2N)}x_t$ , with  $x_t\in\{\pm 1\pm j\}^N$ , represents the complex baseband one-bit transmitted signal;  $v_{i,t}$  is noise and is assumed to be i.i.d. circular complex Gaussian with mean zero and variance  $\sigma_v^2$ .

The BS aims to transmit parallel data symbols to the users. Let  $s_{i,t} \in \mathcal{S}$  denote the symbol to be transmitted to the ith user at symbol time t, where  $\mathcal{S}$  denotes the symbol constellation set. For convenience, we will assume that

$$\max_{s \in \mathcal{S}} |s| = 1;$$

or, the symbol constellation is normalized such that the above equation holds. The challenge is to find  $x_t \in \{\pm 1 \pm j\}^N$ , for  $t = 1, \ldots, T$ , such that

$$\boldsymbol{h}_{i}^{T} \boldsymbol{x}_{t} \approx c_{i,t} s_{i,t}, \quad \text{for all } i, t,$$
 (2)

where  $c_{i,t} > 0$  denotes a scaling factor. In words, we aim to shape the symbols at the user side under the one-bit transmitted signal constraints; see [1] for further discussions of  $c_{i,t}$  for PSK and QAM. We are interested in the single-path angular array channel. Each  $\boldsymbol{h}_i$  is characterized as

$$\boldsymbol{h}_i = \alpha_i \boldsymbol{a}(\theta_i), \tag{3}$$

where  $\alpha_i \in \mathbb{C}$  is the complex channel gain;  $\theta_i \in [-\pi/2, \pi/2]$  denotes the angle of departure from the BS to the *i*th user;

$$\boldsymbol{a}(\theta) = \left[1, e^{-j\frac{2\pi d}{\lambda}\sin(\theta)}, \dots, e^{-j(N-1)\frac{2\pi d}{\lambda}\sin(\theta)}\right]^T \tag{4}$$

denotes the array response vector at  $\theta$ , in which  $\lambda$  is the carrier wavelength and  $d \leq \lambda/2$  is the inter-antenna spacing.

### 3. BASICS OF $\Sigma\Delta$ MODULATION

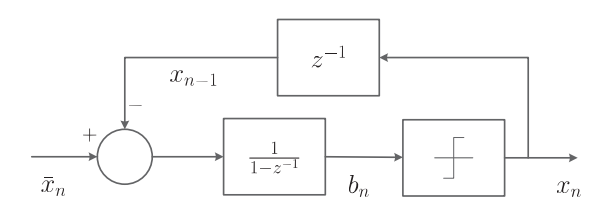


**Fig. 1**: The first-order  $\Sigma\Delta$  modulator.

This section reviews the basic concepts of  $\Sigma\Delta$  modulation. Consider the the first-order  $\Sigma\Delta$  modulator in Fig. 1. We have a discrete-time real-valued signal sequence  $\{\bar{x}_n\}_{n\in\mathbb{Z}_+}$  as the modulator input. In the application of temporal DACs,  $\bar{x}_n$  is a significantly oversampled version of some signal. Here, it is sufficient to know that  $\bar{x}_n$  is a low-pass signal. The problem is to one-bit quantize  $\{\bar{x}_n\}_n$  in a way that the resulting quantization noise is high-pass. Doing so satisfactorily will result in negligible quantization noise effects on

the low-pass frequency region of the desired signal  $\bar{x}_n$ . The  $\Sigma\Delta$  modulator output sequence, denoted by  $\{x_n\}_{n\in\mathbb{Z}_+}$ , is generated as

$$x_n = \operatorname{sgn}(b_n), \tag{5a}$$

$$b_n = b_{n-1} + (\bar{x}_n - x_{n-1}), \tag{5b}$$

for  $n=0,1,\ldots$ , and with  $b_{-1}=x_{-1}=0$ . Let  $q_n=x_n-b_n$ ,  $n\in\mathbb{Z}_+$ , denote the quantization noise, and let  $q_{-1}=0$  for convenience. From (5) one can show that

$$x_n = \bar{x}_n + q_n - q_{n-1}, \quad n \in \mathbb{Z}_+,$$

and subsequently

$$X(z) = \bar{X}(z) + (1 - z^{-1})Q(z),$$

where  $X(z) = \sum_{n=0}^{\infty} x_n z^{-n}$  denotes the z-transform. The high-pass response  $1-z^{-1}$  suppresses the quantization noise at low frequency.

A key issue in  $\Sigma\Delta$  modulation is the effect of overloading. Overloading refers to the situation when the quantizer input  $b_n$  has amplitude greater than 2. The consequence is that the corresponding quantization noise  $q_n$  goes beyond the range [-1,1]. As an example of showing what problem overloading can bring, consider

$$\bar{x}_n = 1 + \epsilon$$
, for all  $n \in \mathbb{Z}_+$ ,

where  $\epsilon>0$ . This is an instance in which the signal amplitude is greater than one. One can verify from (5) that  $b_n=1+(n+1)\epsilon$  and  $q_n=-(n+1)\epsilon$ . We see that the quantization noise is unbounded as  $n\to\infty$ . A sufficient condition under which overloading can be safely avoided is to limit the input signal range as

$$-1 \le \bar{x}_n \le 1$$
, for all  $n \in \mathbb{Z}_+$ . (6)

Under the above condition it is guaranteed that  $|b_n| \leq 2$  for all  $n \in \mathbb{Z}_+$ , and consequently,

$$-1 \le q_n \le 1$$
, for all  $n \in \mathbb{Z}_+$ .

Under the no-overload condition (6), it is very common to assume that the quantization noise  $q_n$  is i.i.d., uniformly distributed on [-1,1], and independent of  $\{\bar{x}_n\}$ . This assumption is widely adopted for signal-to-quantization-noise ratio (SQNR) prediction in the  $\Sigma\Delta$ -DAC/ADC literature [29].

# 4. SPATIAL $\Sigma\Delta$ MODULATION

We now present the spatial  $\Sigma\Delta$  modulation approach. For notational simplicity, we remove the time index t from (1) and write

$$y_i = \sqrt{\frac{P}{2N}} \boldsymbol{h}_i^T \boldsymbol{x} + v_i. \tag{7}$$

Also, with a slight abuse of notation, let  $\bar{x}=[\bar{x}_1,\ldots,\bar{x}_N]^T$  be the signal we wish to  $\Sigma\Delta$ -modulate. We apply first-order  $\Sigma\Delta$  modulation (as described in the preceding section) to  $\{\bar{x}_n\}_{n=1}^N$  to obtain  $\{x_n\}_{n=1}^N$ . The resulting  $x=[x_1,\ldots,x_N]^T$  then serves as the one-bit transmitted signal. More precisely, we use two first-order  $\Sigma\Delta$  modulators, one for the real part and another for the imaginary part, to get x. To avoid overloading, we restrict  $-1 \leq \Re(\bar{x}_n) \leq 1$  and  $-1 \leq \Im(\bar{x}_n) \leq 1$  for all n. By doing so, we perform  $\Sigma\Delta$  modulation in space.

Following the preceding section, we can write

$$x = \bar{x} + q - q^{-} \tag{8}$$

where  $\mathbf{q} = [q_1, q_2 \dots, q_N]^T$ ;  $\mathbf{q}^- = [0, q_1, \dots, q_{N-1}]^T$ ; each  $q_i$  is complex quantization noise with  $-1 \leq \Re(q_n) \leq 1$  and  $-1 \leq \Im(q_n) \leq 1$  (this is guaranteed when  $-1 \leq \Re(\bar{x}_n) \leq 1$ ). For the sake of analysis, we model the  $q_n$ 's as i.i.d. uniform noise on the unit box interval  $\{q = a + \mathrm{j}b \mid a, b \in [-1, 1]\}$ . Putting (8) into (7) gives

$$y_i = \sqrt{\frac{P}{2N}} \boldsymbol{h}_i^T \bar{\boldsymbol{x}} + w_i, \tag{9a}$$

$$w_i = \sqrt{\frac{P}{2N}} \boldsymbol{h}_i^T (\boldsymbol{q} - \boldsymbol{q}^-) + v_i, \tag{9b}$$

where  $w_i$  combines quantization noise and background noise. We are interested in knowing how the noise power scales with the system parameters. Let  $z_i = e^{j\frac{2\pi d}{\lambda}\sin(\theta_i)}$  for convenience. We see that

$$\boldsymbol{a}_{i}^{T}(\boldsymbol{q}-\boldsymbol{q}^{-})=(1-z_{i}^{-1})\sum_{n=0}^{N-2}z_{i}^{-n}q_{n+1}+z_{i}^{-(N-1)}q_{N},$$

and consequently,  $\mathbb{E}[oldsymbol{a}_i^T(oldsymbol{q}-oldsymbol{q}^-)]=0$  and

$$\mathbb{E}[|\boldsymbol{a}_i^T(\boldsymbol{q} - \boldsymbol{q}^-)|^2] = |1 - z_i^{-1}|^2(N - 1)\sigma_q^2 + \sigma_q^2,$$

where  $\sigma_q^2=\mathbb{E}[|q_n|^2]=2/3$  due to the assumption of uniform i.i.d. quantization noise. It follows that  $\mathbb{E}[w_i]=0$  and

$$\sigma_{w,i}^2 = \mathbb{E}[|w_i|^2] = \frac{|\alpha_i|^2 P}{3N} (|1 - z_i^{-1}|^2 (N - 1) + 1) + \sigma_v^2.$$

By assuming large N, the above quantization noise variance formula can be simplified to

$$\sigma_{w,i}^2 \approx \frac{|\alpha_i|^2 P}{3} |1 - z_i^{-1}|^2 + \sigma_v^2$$
 (10a)

$$= \frac{4|\alpha_i|^2 P}{3} \left| \sin\left(\frac{\pi d}{\lambda}\sin(\theta_i)\right) \right|^2 + \sigma_v^2.$$
 (10b)

Eq. (10b) reveals interesting behaviors with the quantization noise effects at the user side.

- 1. First, the quantization noise power increases as the absolute value of the angle  $|\theta|$  increases; broadside  $(\theta=0)$  is the best, while endfire  $(\theta=\pi/2 \text{ or } \theta=-\pi/2)$  is the worst. This suggests that spatial  $\Sigma\Delta$  modulation serves users with smaller  $|\theta|$  better. An illustrative example showing the  $\Sigma\Delta$ -modulated signal angular power spectrum is presented later in Section 6. Here we also draw connections between conventional  $\Sigma\Delta$  modulation for discrete-time signals and the spatial  $\Sigma\Delta$  modulation proposed above. Simply speaking, frequency in the temporal case becomes angle in the spatial case.  $\Sigma\Delta$  modulation in time and space serve low frequency and low angle signals better, respectively.
- 2. Second, the quantization noise power decreases as we decrease the inter-antenna spacing *d*. This means that we may want to employ more densely spaced antennas. In practice, however, it is infeasible to have very small inter-antenna spacing as that will introduce strong mutual coupling effects. Also, the physical dimensions of the antennas prevent small spacing. We will have to rely on large *N* and smaller operating angular ranges to reduce the quantization noise.
- 3. Third, the quantization noise power at the user side is independent of the number of antennas N. This will give us substantial advantages in using massive MIMO to suppress the quantization noise, as we will further show in the next section.

#### 5. $\Sigma\Delta$ ZERO-FORCING

This section proposes a ZF precoder under spatial  $\Sigma\Delta$  modulation. For notational convenience, define

$$\|\boldsymbol{x}\|_{IQ-\infty} = \max\{|\Re(x_1)|, |\Im(x_1)|, \dots, |\Re(x_N)|, |\Im(x_N)|\};$$

that is, the infinity norm applied on the in-phase and quadrature-phase components of a vector. Also, assume M-ary PSK constellations. The ZF precoding scheme implements

$$\bar{x} = \gamma A^{\dagger} D s, \tag{11}$$

where  $s \in \mathcal{S}^K$  is the symbol vector, with  $s_i$  representing the symbol for the ith user;

$$D = \text{Diag}(\sigma_{w,1}\alpha_1^*/|\alpha_1|^2, \dots, \sigma_{w,K}\alpha_K^*/|\alpha_K|^2),$$
  

$$A = [a_1, \dots, a_K]^T, \quad a_i = a(\theta_i);$$

and  $\gamma$  is a normalization constant such that  $\|\bar{x}\|_{IQ-\infty}=1.$  It is easy to see that

$$\gamma = \frac{1}{\|\mathbf{A}^{\dagger} \mathbf{D} \mathbf{s}\|_{IQ-\infty}}.$$
 (12)

This ZF precoding scheme is designed such that every user has the same effective SNR, and consequently, uniform SEP performance. To see this, consider putting (11) into (9). It can be shown that

$$y_i = c_i \cdot s_i + w_i, \quad c_i = \sqrt{\frac{P}{2N}} \gamma \sigma_{w,i}.$$

The effective SNR of the ith user is

$$\mathsf{SNR}_{\mathsf{eff},i} = \frac{c_i^2}{\sigma_{m,i}^2} = \frac{P}{2N} \gamma^2. \tag{13}$$

Clearly, the effective SNRs of all the users are identical. How the effective SNRs scale with the system parameters is shown as follows:

**Proposition 1** Consider the  $\Sigma\Delta$  ZF precoding scheme described above. Let  $k = \arg\max_{i=1,...,K} \sigma_{w,i}/|\alpha_i|$ . The users' effective SNRs are bounded by

$$\mathsf{SNR}_{\mathsf{eff},i} \ge \frac{PN|\alpha_k|^2 \lambda_{\min}^2(\boldsymbol{R})}{2K^3 \left(\frac{4|\alpha_k|^2 P}{3} \left| \sin\left(\frac{\pi d}{\lambda}\sin(\theta_k)\right) \right|^2 + \sigma_v^2 \right)},\tag{14}$$

for all i, where  $\mathbf{R} = \mathbf{A}\mathbf{A}^H/N$ ;  $\lambda_{\min}(\mathbf{R})$  denotes the smallest eigenvalue of  $\mathbf{R}$ . Also, it holds that

$$1 \ge \lambda_{\min}(\mathbf{R}) \ge 1 - (K - 1)\rho,\tag{15}$$

where

$$\rho = \max_{i \neq j} \left| D_N \left( \frac{\pi d}{\lambda} (\sin(\theta_i) - \sin(\theta_j)) \right) \right|,$$

and  $D_N(\phi) = \sin(N\phi)/(N\sin(\phi))$  is the digital sinc function.

The proof of proposition 1 can be found in the journal version of this paper [1]. Let us discuss the implications of the theoretical result in (14)–(15). First, the quantization noise effect increases with the absolute value of the angle. Second, the lower bound of the effective SNRs increases linearly with the number of antennas N, which suggests that  $\Sigma\Delta$  precoding is favorable for massive MIMO. Third,  $\lambda_{\min}(\mathbf{R})$ , which appears in the signal power part of the effective SNR, is large if the user angles are well separated, but small if some of the angles are close. This factor is relative to N. Fixing the angles, larger N brings  $\lambda_{\min}(\mathbf{R})$  closer to its largest value, 1.

#### 6. SIMULATION RESULTS

This section presents some representative simulation results for spatial  $\Sigma\Delta$  modulation. First, we consider the PSK case. Fig. 2 shows the angular power spectrum  $\mathbb{E}[\|\boldsymbol{a}(\psi)\boldsymbol{x}\|^2]$  on  $[-90^\circ,90^\circ]$  for  $\Sigma\Delta$  ZF. There are N=256 antennas at the BS with spacing  $d=\lambda/4$ ; the complex channel gain  $\alpha_i$ 's are generated by  $|\alpha_i|=1$  and phases uniformly drawn on  $[-\pi,\pi]$ ; there are three users with angles  $-10^\circ$ ,  $0^\circ$  and  $5^\circ$ ; we also assume no background noise in this case, i.e.,  $\sigma_v^2=0$ ; 8-ary PSK is used in the simulation. In Fig. 2, it is seen that the angular spectrum of  $\Sigma\Delta$  ZF comprises three sharp peaks at the user angles and a high-pass response for the quantization noise. This result is in agreement with the theoretical analysis in (10).

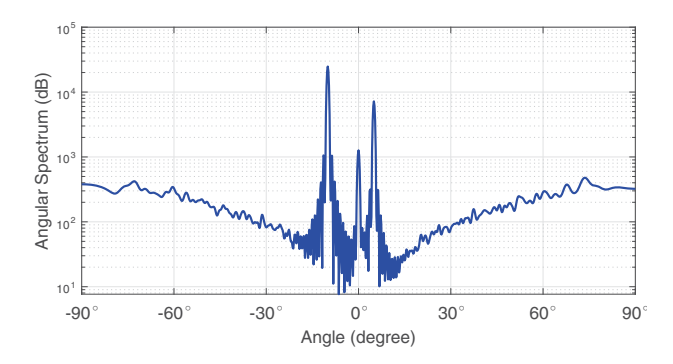


**Fig. 2**: An illustration of the angular power spectrum of first-order  $\Sigma \Delta$  ZF

Next we consider the bit-error rate (BER) of the massive MISO system. The simulation settings are as follows: The number of antennas is N=256; the inter-antenna spacing is  $d=\lambda/8$ ; the number of users is K=24, and the users lie within an angular range  $[-22.5^{\circ}, 22.5^{\circ}]$ ; the angles  $\theta_i$  of the users are randomly chosen from the interval  $[-22.5^{\circ}, 22.5^{\circ}]$  with inter-angle difference no less than  $1^{\circ}$ ; the complex channel gains  $\alpha_i$  have phases uniformly drawn from  $[-\pi,\pi]$ , and their amplitudes are generated as  $|\alpha_i|=r_0/r_i$  where  $r_0=30$  and the  $r_i$  are uniformly drawn from [20,100] (this is a standard free-space path-loss model, with  $r_i$  being the distance from the BS to the ith user and  $r_0$  being a reference value); the symbol constellation is 8-ary PSK.

Fig. 3 shows the results. The algorithms compared are the SQUID algorithm [13] and the maximum safety margin (MSM) algorithm [16]. In the legend, "unquant. ZF" is the unquantized ZF scheme under the average power constraint; "quant. ZF" is the direct one-bit quantization of the unquantized ZF scheme; " $\Sigma\Delta$  ZF" is the  $\Sigma\Delta$  ZF scheme. We also show the result of the nullspace-assisted  $\Sigma\Delta$  ZF scheme, which takes advantage of the nullspace of the channel matrix to further improve the performance of  $\Sigma\Delta$  ZF; see [1] for details. We see that both the proposed  $\Sigma\Delta$  ZF and the nullspace-assisted  $\Sigma\Delta$  ZF schemes work better than the directly quantized ZF. Also, the nullspace-assisted  $\Sigma\Delta$  ZF performs much better than MSM and SQUID at high SNRs.

Finally, we consider the BER for the QAM case. The simulation settings are: 16-ary QAM, N=256,~K=16, and transmission block length T=100. Also, the angular range is  $[-30^\circ,30^\circ]$ , and the  $\alpha_i$ 's are generated as before. Fig. 4 shows the results. The  $\Sigma\Delta$  ZF and  $\Sigma\Delta$  nullspace-assisted ZF for QAM follow [1, Section 5.C]. "GEMM" is the direct one-bit precoding design in [19]. We see that the  $\Sigma\Delta$  ZF schemes, with and without nullspace assistance, achieve good performance. Also we see that the nullspace-assisted  $\Sigma\Delta$  ZF

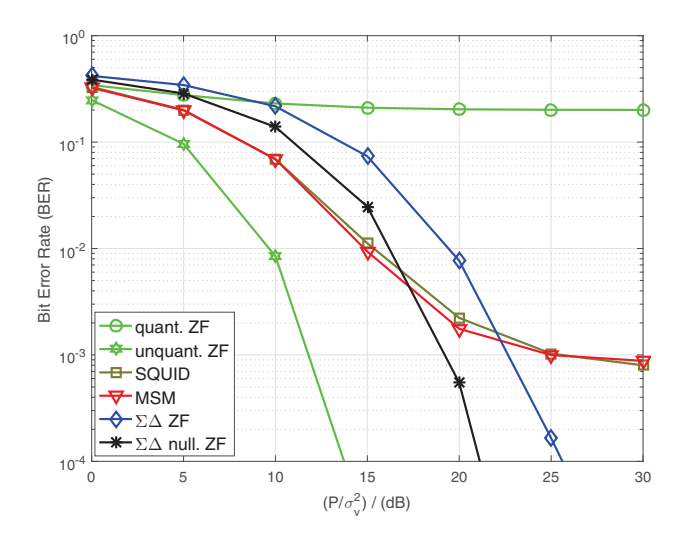
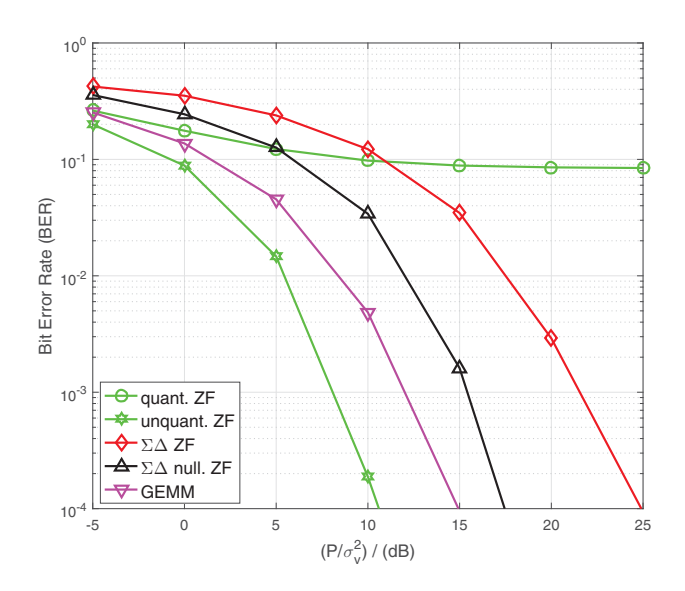


Fig. 3: BERs of the multi-user  $\Sigma\Delta$  precoding schemes in the 8-ary PSK case.



**Fig. 4**: BERs of the multi-user  $\Sigma\Delta$  precoding schemes in the 16-ary QAM case.

scheme achieves a 5dB gain compared to the  $\Sigma\Delta$  ZF approach, and it is only 3dB away from GEMM, which requires a significantly higher optimization complexity than the nullspace-assisted  $\Sigma\Delta$  ZF approach.

# 7. CONCLUSION

This paper studied the potential of spatial  $\Sigma\Delta$  modulation for one-bit massive MIMO precoding. By implementing the BS with a uniform linear array and one-bit DACs,  $\Sigma\Delta$  modulation is able to substantially reduce the quantization noise effects for users with signals that are received near the broadside of the array. Our analysis and simulations showed that spatial  $\Sigma\Delta$  modulation favors large antenna arrays, and thus is compatible with massive MIMO. Empirical results showed that the proposed  $\Sigma\Delta$  ZF approach can achieve much better performance than directly quantized ZF precoding.

#### 8. REFERENCES

- [1] M. Shao, W. Ma, Q. Li, and A. L. Swindlehurst, "One-bit sigma-delta MIMO precoding," *IEEE J. Sel. Topics Signal Process.*, vol. 13, no. 5, pp. 1046–1061, Sep. 2019.
- [2] L. Fan, S. Jin, C. Wen, and H. Zhang, "Uplink achievable rate for massive MIMO systems with low-resolution ADC," *IEEE Commun. Lett.*, vol. 19, no. 12, pp. 2186–2189, Dec 2015.
- [3] J. Choi, J. Mo, and R. W. Heath, "Near maximum-likelihood detector and channel estimator for uplink multiuser massive MIMO systems with one-bit ADCs," *IEEE Trans. Commun.*, vol. 64, no. 5, pp. 2005–2018, May 2016.
- [4] C. Mollén, J. Choi, E. G. Larsson, and R. W. Heath, "Uplink performance of wideband massive MIMO with one-bit ADCs," *IEEE Trans. Wireless Commun.*, vol. 16, no. 1, pp. 87–100, Jan 2017
- [5] Y. Li, C. Tao, G. Seco-Granados, A. Mezghani, A. L. Swindlehurst, and L. Liu, "Channel estimation and performance analysis of one-bit massive MIMO systems," *IEEE Trans. Signal Process.*, vol. 65, no. 15, pp. 4075–4089, Aug 2017.
- [6] S. Jacobsson, G. Durisi, M. Coldrey, U. Gustavsson, and C. Studer, "Throughput analysis of massive MIMO uplink with low-resolution ADCs," *IEEE Trans. Wireless Commun.*, vol. 16, no. 6, pp. 4038–4051, June 2017.
- [7] Z. Shao, R. C. de Lamare, and L. T. N. Landau, "Iterative detection and decoding for large-scale multiple-antenna systems with 1-bit ADCs," *IEEE Wireless Commun. Lett.*, vol. 7, no. 3, pp. 476–479, June 2018.
- [8] Y. Jeon, N. Lee, S. Hong, and R. W. Heath, "One-bit sphere decoding for uplink massive MIMO systems with one-bit ADCs," *IEEE Trans. Wireless Commun.*, vol. 17, no. 7, pp. 4509–4521, July 2018.
- [9] A. Mezghani, R. Ghiat, and J. A. Nossek, "Transmit processing with low resolution D/A-converters," in *Proc. 16th IEEE Int. Conf. Electron., Circuits, Syst.*, Dec 2009, pp. 683–686.
- [10] A. K. Saxena, I. Fijalkow, and A. Swindlehurst, "Analysis of one-bit quantized precoding for the multiuser massive MIMO downlink," *IEEE Trans. Signal Process.*, vol. 65, no. 17, pp. 4624–4634, Sept 2017.
- [11] Y. Li, C. Tao, A. L. Swindlehurst, A. Mezghani, and L. Liu, "Downlink achievable rate analysis in massive MIMO systems with one-bit DACs," *IEEE Commun. Lett.*, vol. 21, no. 7, pp. 1669–1672, July 2017.
- [12] O. Castaneda, S. Jacobsson, G. Durisi, M. Coldrey, T. Goldstein, and C. Studer, "1-bit massive MU-MIMO precoding in VLSI," *IEEE J. Emerg. Sel. Topics Circuits Syst.*, vol. 7, no. 4, pp. 508–522, Dec 2017.
- [13] S. Jacobsson, G. Durisi, M. Coldrey, T. Goldstein, and C. Studer, "Quantized precoding for massive MU-MIMO," *IEEE Trans. Commun.*, vol. 65, no. 11, pp. 4670–4684, Nov 2017.
- [14] A. Swindlehurst, A. Saxena, A. Mezghani, and I. Fijalkow, "Minimum probability-of-error perturbation precoding for the one-bit massive MIMO downlink," in *Proc. IEEE Int. Conf. Acous., Speech, Signal Process. (ICASSP)*, Mar. 2017, pp. 6483–6487.

- [15] L. T. N. Landau and R. C. de Lamare, "Branch-and-bound precoding for multiuser MIMO systems with 1-bit quantization," *IEEE Wireless Commun. Lett.*, vol. 6, no. 6, pp. 770–773, Dec 2017.
- [16] H. Jedda, A. Mezghani, A. L. Swindlehurst, and J. A. Nossek, "Quantized constant envelope precoding with PSK and QAM signaling," *IEEE Trans. Wireless Commun.*, vol. 17, no. 12, pp. 8022–8034, Dec 2018.
- [17] A. Li, C. Masouros, F. Liu, and A. L. Swindlehurst, "Massive MIMO 1-bit DAC transmission: A low-complexity symbol scaling approach," *IEEE Trans. Wireless Commun.*, vol. 17, no. 11, pp. 7559–7575, 2018.
- [18] F. Sohrabi, Y.-F. Liu, and W. Yu, "One-bit precoding and constellation range design for massive MIMO with QAM signaling," *IEEE J. Sel. Topics Signal Process.*, vol. 12, no. 3, pp. 557–570, 2018.
- [19] M. Shao, Q. Li, W.-K. Ma, and A. M.-C. So, "A framework for one-bit and constant-envelope precoding over multiuser massive MISO channels," *IEEE Trans. Signal Process.*, vol. 67, no. 20, pp. 5309–5324, 2019.
- [20] P. M. Aziz, H. V. Sorensen, and J. Van Der Spiegel, "An overview of sigma-delta converters: How a 1-bit ADC achieves more than 16-bit resolution," *IEEE Signal Process. Mag.*, vol. 13, no. 1, pp. 61–84, 1996.
- [21] R. M. Corey and A. C. Singer, "Spatial sigma-delta signal acquisition for wideband beamforming arrays," in *Proc. Int. ITG* Workshop Smart Antennas (WSA), March 2016.
- [22] D. Barac and E. Lindqvist, "Spatial sigma-delta modulation in a massive MIMO cellular system," Master's thesis, Department of Computer Science and Engineering, Chalmers University of Technology, 2016.
- [23] A. Nikoofard, J. Liang, M. Twieg, S. Handagala, A. Madanayake, L. Belostotski, and S. Mandal, "Low-complexity N-port ADCs using 2-D sigma-delta noise-shaping for N-element array receivers," in *Proc. Int. Midwest Sympo-sium Circuits Syst. (MWSCAS)*, 2017, pp. 301–304.
- [24] A. Madanayake, N. Akram, S. Mandal, J. Liang, and L. Belostotski, "Improving ADC figure-of-merit in wideband antenna array receivers using multidimensional space-time delta-sigma multiport circuits," in *Proc. Int. Workshop Multidimensional (nD) Syst. (nDS)*, Sept 2017.
- [25] S. Rao, A. L. Swindlehurst, and H. Pirzadeh, "Massive MIMO channel estimation with 1-bit spatial sigma-delta ADCs," in *Proc. IEEE Int. Conf. Acous., Speech, Signal Process.* (ICASSP). IEEE, 2019, pp. 4484–4488.
- [26] H. Pirzadeh, G. Seco-Granados, S. Rao, and A. L. Swindlehurst, "Spectral efficiency of one-bit sigma-delta massive MIMO," arXiv preprint arXiv:1910.05491, 2019.
- [27] D. P. Scholnik, J. O. Coleman, D. Bowling, and M. Neel, "Spatio-temporal delta-sigma modulation for shared wideband transmit arrays," in *Proc. IEEE Radar Conf.*, 2004, pp. 85–90.
- [28] J. D. Krieger, C. P. Yeang, and G. W. Wornell, "Dense deltasigma phased arrays," *IEEE Trans. Antennas Propag.*, vol. 61, no. 4, pp. 1825–1837, April 2013.
- [29] R. M. Gray, "Quantization noise spectra," *IEEE Trans. Inf. Theory*, vol. 36, no. 6, pp. 1220–1244, 1990.